CrossMark
click for updates

Side-chain poly(phosphoramidate)s *via* acyclic diene metathesis polycondensation†

Alper Cankaya, Mark Steinmann, Yagmur Bülbül, Ingo Lieberwirth and Frederik R. Wurm*

Poly(phosphoester)s (PPEs) are interesting degradable multi-functional polymers. Here, we present the first synthesis of poly(phosphoramidate)s (PPAs) *via* acyclic diene metathesis (ADMET) polycondensation with amidate linkages in side chains. In contrast to conventional polyamides, the P–N-bond in phosphoramidates is more labile than the corresponding esters. Unsaturated PPAs were compared with structural analogues of PPEs: two novel α,ω-dienes, *i.e.* bis-(undecen-10-yl)-*n*-butyl-phosphoramidate (**1**) and bis-(undecen-10-yl)-*n*-butyl-phosphate (**2**) have been polymerized by Grubbs-type catalysts to polymers with molecular weights up to *ca.* 20 000 g mol^{-1}. After hydrogenation polyethylene-like structures were obtained with the phosphoramidate or -ester representing a precisely placed defect. PPAs were compared to their PPE analogues with respect to their thermal behavior and stability by differential scanning calorimetry (DSC) and thermogravimetric analysis (TGA), showing similar crystallization behavior for the saturated materials, but significant differences for unsaturated PPA *vs.* PPE. This synthesis of PPAs *via* ADMET polymerization offers an interesting approach to various PPAs. The hydrolytically labile pendant phosphoramidate further offers the possibility for the development of hydrolytically degradable materials or as processable intermediates for poly(phosphodiester)s which often show limited solubility.

Introduction

Biodegradable polymers with precise properties and structures are a field of research with increasing attention ranging from plastics to biomedical implants or drug delivery, for example. Polyesters and -amides lead the field in current literature due to established syntheses and have proven biocompatibility.[1,2] However, as polyesters degrade, the pH may drop due to the release of carboxylic acids; also the chemical versatility of polyesters is limited or may demand several reaction steps to introduce functionality.[3]

Poly(phosphoester)s (PPEs), with a backbone of repeating phosphoester bonds, are biodegradable and (typically) biocompatible polymers with a high degree of chemical versatility.[4] Due to the formation of three ester-bonds, PPEs can be tailored along their main and side chains,[5] offering a variety of possible polymer structures, making PPEs interesting for diverse applications like for drug[6–8] and gene delivery[9] and tissue engineering.[10] The stability of the phosphorus-containing polymers is directly influenced by the first binding sphere around the central phosphorus: the development of poly(phosphonate)s with a stable P–C-bond as the main[11] or side chain elements[12] or poly(phosphoramidate)s (PPAs) with a hydrolysis-labile P–N bond in the side chain[13] has a direct influence on the polymers' degradation profile.

Side-chain PPAs have been only scarcely studied; their classical synthesis relies on the post-polymerization modification of poly(H-phosphonate)s by the versatile Atherton–Todd reaction.[14–16] More recently, the Wooley lab presented an elegant approach by ring-opening polymerization[13] of cyclic dioxaphospholane. PPAs have been studied for the delivery of nucleic acids or as flame-retardant polymers.[2,14,17–19]
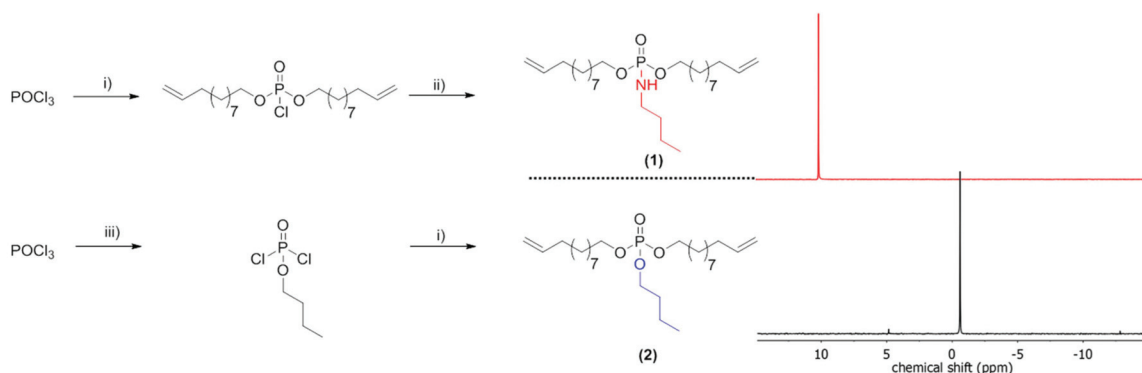
Our group developed several protocols based on olefin metathesis polymerization (either as acyclic diene metathesis (ADMET) or ring-opening metathesis polymerization) for phosphorus-containing materials.[20–22]

Herein, we use the robust ADMET protocol[23] to present the first strategy to aliphatic saturated and unsaturated PPAs with the phosphoramidate bond in the side chain. The labile P–N bond can be used to release the pendant chain (*e.g.* for pH-sensitive drug delivery) or can be regarded as a soluble precursor for poly(phosphodiester)s after acidic hydrolysis, which typically are hardly soluble and are interesting materials for bone targeting, for example.[24] Such polymers may also find useful application as novel polymeric flame retardant additives.[25] In addition, we compare the PPA to a structurally identical PPE (a single oxygen is exchanged by "NH", *cf.* Scheme 1).

Max-Planck-Institut für Polymerforschung, Ackermannweg 10, 55128 Mainz, Germany. E-mail: wurm@mpip-mainz.mpg.de

Scheme 1 Synthesis of the ADMET monomers bis-(undecen-10-yl) butylphosphoramidate (**1**) and bis-(undec-10-en-1-yl)butylphosphate (**2**) and their ^{31}P NMR spectra. (i) 10-undecen-1-ol, triethylamine, dichloromethane; (ii) butylamine, triethylamine, dichloromethane; (iii) butanol, triethylamine, dichloromethane.

Experimental

Materials

Solvents were purchased from Acros Organics and Sigma Aldrich and used as received, unless otherwise stated. Phosphoroxychloride, 10-undecen-1-ol, triethylamine, tris(hydroxymethyl)phosphine and butan-1-ol were used as received from Sigma-Aldrich (Germany). The 1st generation Grubbs catalyst was purchased from Sigma-Aldrich and stored under an argon atmosphere. *n*-Butyl amine was purchased from TCI chemicals and used without further purification. Deuterated solvents were purchased from Acros Organics and Carl Roth Chemicals.

Instrumentation

Gel-permeation chromatography (GPC) measurements were carried out in THF, with samples of the concentration of 1 g L^{-1}. Sample injection was performed by using a 1260-ALS auto sampler (Waters) at 30 °C (THF). The flow rate was 1 mL min^{-1}. In THF, three SDV columns (PSS) with dimensions of 300 × 80 mm, 10 μm particle size and pore sizes of 106, 104 und 500 Å were employed. Detection was accomplished with a DRI Shodex RI-101 detector (ERC) and UV-vis 1260-VWD detector (Agilent). Calibration was achieved *vs.* poly(styrene) standards provided by Polymer Standards Service. ^{1}H-NMR spectra were recorded on a Bruker Avance 300 MHz spectrometer, ^{13}C-NMR and ^{31}P-spectra were recorded on a Bruker Avance III 500 MHz spectrometer. [1]H[15]N-NMR spectra were recorded on a Bruker Avance 700 III MHz spectrometer. The ^{13}C-NMR (176 MHz) and ^{31}P-NMR (283 MHz) measurements were obtained with a ^{1}H powergate decoupling method using a 30° degree flip angle.

[1]H-DOSY experiments were recorded with a 5 mm BBI 1H/X *z*-gradient on a 700 MHz spectrometer with a Bruker Avance III system. For a ^{1}H NMR spectrum 64 transients were used with an 11 μs long 90° pulse and a 12 600 Hz spectral width together with a recycling delay of 5 s. The temperature for all experiments was kept at 298.3 K. For the diffusion measurements a 2D sequence (DOSY[1], dstebgp3s[2]) with a double stimulated echo for convection compensation and LED using a

bipolar gradient pulse for diffusion was used additionally.[26] The temperature was maintained at 298.3 K and regulated by using a standard ^{1}H methanol NMR sample using the topspin 3.2 software (Bruker). The control of the temperature was realized with a VTU (variable temperature unit) and with an accuracy of ±0.1 K.

The proton, carbon and phosphorous spectra were measured in CDCl$_3$ or DMSO-d_6. The spectra were referenced to the residual proton signals of the deuterated solvent (CDCl$_3$ (^{1}H) = 7.26 ppm; DMSO-d_6 (^{1}H) = 2.50 ppm). All spectra were processed with MestReNova 6.1.1-6384 software. Differential Scanning Calorimetry (DSC) measurements were performed using a Perkin-Elmer 7 series thermal analysis system and a Perkin Elmer Thermal Analysis Controller TAC 7/DX in the temperature range from −150 to 130 °C. Three scanning cycles of heating–cooling were performed (in a N$_2$ atmosphere 30 mL min^{-1}) at a heating rate of 10 °C min^{-1}.

Thermogravimetric analysis (TGA) was performed on Mettler Toledo ThermoSTAR TGA/SDTA 851-Thermowaage in the range of temperature between 25 °C and 600 °C, at a heating rate of 10 °C min^{-1}. For wide-angle X-ray scattering (WAXS) and small-angle X-ray scattering (SAXS) experiments samples were prepared by hot pressing an approximately 200–400 μm thick film on a hot stage. A sufficient amount of the sample was placed on a preheated glass slide and allowed to melt. Subsequently, another hot glass slide was pressed on the melt. This sandwich was kept above the melting point for another 5 min before cooling it down to room temperature in order to eliminate any shear-induced orientation in the sample.

SAXS was recorded using CuKα radiation (wavelength 1.54 Å) from a rotating anode source (Rigaku MicroMax 007 X-ray generator) with curved multilayer optics (Osmic Confocal Max-Flux). The scattered intensity was recorded on a 2D detector (Mar345 image plate) with a sample–detector distance of 2 m. For WAXS measurements the sample–detector distance was set to 20 cm. For Transmission Electron Microscopy (TEM), a FEI Tecnai F20 transmission electron microscope operating at an acceleration voltage of 200 kV was used to

determine the crystal morphology, thickness, and crystal structure.

Synthesis of bis-(undecen-10-yl) chlorophosphate. To a dried two-necked, 500 mL round bottom flask, 5 g (32.61 mmol) phosphoroxychloride dissolved in 100 mL of dry CH_2Cl_2 were added under an argon atmosphere. After cooling down the solution to 0 °C, 1.8 equiv. (58.70 mmol) of 10-undecen-1-ol and 1 equiv. (3.3 g, 32.61 mmol) of triethylamine dissolved in 50 mL CH_2Cl_2 were added drop-wise to the solution at 0 °C. The reaction was stirred overnight at room temperature. The precipitated $Et_3N·HCl$ was removed as a white solid by filtration, the filtrate was reduced at reduced pressure. The residue was dissolved in diethylether and further precipitated $Et_3N·HCl$ was removed again. This procedure was repeated until no further salt precipitation occurred. After removal of the solvent under reduced pressure a colorless, a viscous liquid was obtained and used for further reactions without purification (Yield: 65%, 21.4 g). ^{1}H-NMR (300 MHz, CDCl₃, ppm): δ 5.81 (ddt, J_1 = 18 Hz, J_2 = 9 Hz, J_3 = 6 Hz, 2H, CH₂=CH–), δ 4.96–4.82 (m, 4H, CH₂=CH–), δ 4.20–3.90 (m, 4H, –O–CH₂–), δ 2.03 (q, J = 6 Hz, 4H, CH₂=CH–CH₂–), δ 1.81–1.71 (m, 4H, –O–CH₂–CH₂–), δ 1.44–1.28 (m, 24H, –CH₂–).

Synthesis of bis-(undecen-10-yl) butylphosphoramidate (1). To a dried two-necked, 250 mL round-bottom flask 8.94 g (21.24 mmol) of bis-(undecen-10-yl) chlorophosphate dissolved in 100 mL of dry CH_2Cl_2 with stirring was added under an argon atmosphere. The solution was cooled to 0 °C, then 1 equiv. of *n*-butylamine (1.55 g, 21.24 mmol) and 1 equiv. of triethylamine (2.15 g, 21.24 mmol) were added drop-wise under cooling to the solution. The reaction was stirred overnight at room temperature. The precipitated $Et_3N·HCl$ was removed as a white solid by filtration, the filtrate was reduced under vacuum. The residue was dissolved in diethylether and further precipitated $Et_3N·HCl$ was removed again. This procedure was repeated until no further salt precipitation occurred. The reduced product was dissolved in CH_2Cl_2 and washed once with aqueous 10% HCl and twice with brine. The organic layer was dried over magnesium sulfate, filtered and concentrated in a vacuum. The product was obtained as a yellow oil after column chromatography over silica using toluene : acetone (8 : 1) as an eluent (R_f: 0.58, yield: 63%, 3.5 g).

^{1}H-NMR (298 K, 300 MHz, DMSO-d_6, ppm): δ 5.81 (ddt, J_1 = 12 Hz, J_2 = 6 Hz, J_3 = 3 Hz 2H, CH₂=CH–), δ 5.02–4.90 (m, 4H, CH₂=CH–), δ 4.79–4.74 (dt, 1H, –NH–), δ 3.97 (qd, 4H, –O–CH₂–), δ 2.92–2.84 (m, 2H, –NH–CH₂–), δ 2.03 (m, =CH–CH₂–), δ 1.65 (q, J = 9 Hz, 4H, –O–CH₂–CH₂–), δ 1.31 (m, 28H, –CH₂–, –CH₂–CH₃), δ 0.91 (t, J = 6 Hz, 3H, –CH₂–CH₃). ^{13}C-NMR (298 K, 75 MHz, DMSO-d_6, ppm): δ 139.06 (CH₂=CH–), 114.04 (CH₂=CH–), 66.21 (–O–CH₂–), 41.06 (–NH–CH₂–), 33.71 (=CH–CH₂–), 30.31 (–O–CH₂–CH₂–), 29.01 (–CH₂–), 25.44 (–NH–CH₂–CH₂–), 19.56 (–CH₂–CH₃), 13.69 (–CH₃). ^{31}P-NMR (298 K, 125 MHz DMSO-d_6, ppm): δ 10.00.

Synthesis of bis-(undec-10-en-1-yl)butylphosphate (2). In a dry three-necked 500 mL round-bottom flask a stirred solution of phosphoroxychloride (6.57 g, 4.00 mL, 42.78 mmol) in 100 mL dry CH_2Cl_2 under an argon atmosphere was cooled down to 0 °C. A mixture of *n*-butanol (5.7 g, 77.01 mmol) and triethylamine (7.79 g, 10.74 mL, 77.01 mmol) in 50 mL dry CH_2Cl_2 was added drop-wise under cooling and stirred overnight at room temperature. In the next step, the reaction mixture was cooled down to 0 °C again and 10-undecen-1-ol (3.17 g, 42.78 mmol) and triethylamine (4.33 g, 42.78 mmol) in 50 mL dry CH_2Cl_2 were added drop-wise to the reaction. The mixture was stirred overnight and $Et_3N·HCl$ was removed as a white solid by filtration. The filtrate was reduced under vacuum. The residue was dissolved in diethylether and further precipitated $Et_3N·HCl$ was removed again. This procedure was repeated until no further salt precipitation occurred. The filtrate was reduced under pressure and dissolved in CH_2Cl_2, washed once with aqueous 10% HCl and twice with brine. The organic layer was dried over magnesium sulfate, filtered and concentrated at reduced pressure. The product was obtained as a yellow oil after column chromatography over silica using dichloromethane : ethylacetate (8 : 1) as an eluent (R_f: 0.8, yield: 37%, 7.4 g).

^{1}H-NMR (298 K, 300 MHz, CDCl₃, ppm): δ 5.74 (ddt, J_1 = 12 Hz, J_2 = 9 Hz, J_3 = 3 Hz, 2H, CH₂=CH–), δ 4.96–4.84 (m, 4H, CH₂=CH–), δ 4.00–3.92 (m, 6H, –O–CH₂–), δ 2.01–1.93 (m, 4H, CH₂=CH–CH₂–), δ 1.65–1.55 (m, 6H, –O–CH₂–), δ 1.36–1.17 (m, 26H, –CH₂–), δ 0.87 (t, J = 6 Hz, 3H, –CH₃). ^{13}C-NMR (298 K, 75 MHz, CDCl₃, ppm): δ 139.09 (CH₂=CH–), 113.93 (CH₂=CH–), 67.45 (–O–CH₂–), 33.66 (=CH–CH₂–), 30.35 (–O–CH₂–CH₂–), 29.15 (–CH₂–), 25.32 (–CH₂–CH₂–CH₃), 18.49 (–CH₂–CH₃), 13.38 (–CH₃). ^{31}P-NMR (298 K, 125 MHz, CDCl₃, ppm): δ −0.65.

Representative procedure for ADMET bulk polycondensation for UPPEs. In a glass Schlenk tube, the monomer (600 mg) and the 1st generation Grubbs catalyst (1–3 mol%) were mixed under an argon atmosphere. The polycondensation was carried out at reduced pressure to remove ethylene gas evolving during the metathesis reaction, at temperatures between 70 °C and 80 °C over a period of 16–18 h. The crude mixture was dissolved in CH_2Cl_2, treated with tris (hydroxymethyl) phosphine (50 eq. with respect to the catalyst) and washed twice with aqueous 10% HCl and water. The organic layer was dried over sodium sulfate, filtered, concentrated at reduced pressure, and precipitated into hexane. Yields were typically between 90–95% (after drying).

P1. ^{1}H-NMR (298 K, 300 MHz, CDCl₃, ppm): δ 5.33–5.25 (m, 2H, –CH=CH–), δ 3.90 (qq, 4H, –O–CH₂–), δ 2.81 (dt, J_1 = 9 Hz, J_2 = 6 Hz, 2H, –NH–CH₂–), δ 1.89 (q, J = 6 Hz, 4H, =CH–CH₂–), δ 1.58 (q, J = 6 Hz, 4H, –O–CH₂–CH₂–), δ 1.42–1.20 (m, 28H, –CH₂–), δ 0.84 (t, J = 6 Hz 3H, –CH₃). ^{13}C-NMR (298 K, 75 MHz, CDCl₃, ppm): δ 130.21 (–CH=CH–), 66.14 (–O–CH₂–), 41.00 (–NH–CH₂–), 33.88 (–CH=CH–CH₂–), 32.61 (–O–CH₂–CH₂–), 30.43 (–CH₂–), 25.60 (–NH–CH₂–CH₂–), 19.74 (–CH₂–CH₃), 13.69 (–CH₃). ^{31}P-NMR (298 K, 125 MHz, CDCl₃, ppm): δ 10.02.

P2. ^{1}H-NMR (298 K, 300 MHz, CDCl₃, ppm): δ 5.33–5.26 (m, 2H, –CH=CH–), δ 3.96 (qd, 6H, –O–CH₂–), δ 1.88 (q, J = 6 Hz, 4H, =CH–CH₂–), δ 1.59 (dtt, 6H, –O–CH₂–CH₂–), δ 1.40–1.20

(m, 26H, $-CH_2-$), δ 0.87 (t, $J = 6$ Hz, 3H, $-CH_3$). ^{13}C-NMR (298 K, 75 MHz, CDCl$_3$, ppm): δ 130.70 ($-CH=CH-$), 68.15 ($-O-CH_2-$), 33.14 ($-CH=CH-CH_2-$), 30.78 ($-O-CH_2-CH_2-$), 30.01 ($-CH_2-$), 25.95 ($-CH_2-CH_3$), 19.15 ($-CH_2-CH_3$), 14.05 ($-CH_3$). ^{31}P-NMR (298 K, 125 MHz, CDCl$_3$, ppm): δ −0.84.

Procedure for the catalytic hydrogenation. In a dried two-necked, 250 mL round-bottom flask, 200 mg of unsaturated polymer in 50 mL toluene and 5% Pd/C (25 mg, 12.5 wt%) were placed and flushed with argon. The mixture was then flushed thoroughly with hydrogen and a hydrogen balloon as a reservoir was connected to the flask. After complete hydrogenation (typically after 36 h) of the polymer the solution was filtered over celite and the polymer was obtained a solid after solvent evaporation in quantitative yield.

P1-H. ^{1}H-NMR (298 K, 300 MHz, CDCl$_3$, ppm): δ 3.93 (qq, 4H, $-O-CH_2-$), δ 2.84 (dt, $J_1 = 9$ Hz, $J_2 = 6$ Hz, 2H, $-NH-CH_2-$), δ 1.58 (q, $J = 7$ Hz, 4H, $-O-CH_2-CH_2-$), δ 1.42–1.20 (m, 28H, $-CH_2-$), δ 0.84 (t, $J = 5$ Hz 3H, $-CH_3$). ^{13}C-NMR (298 K, 75 MHz, CDCl$_3$, ppm): δ 66.14 ($-O-CH_2-$), 41.00 ($-NH-CH_2-$), 32.01 ($-O-CH_2-CH_2-$), 30.43 ($-CH_2-$), 26.20 ($-NH-CH_2-CH_2-$), 19.53 ($-CH_2-CH_3$), 13.71 ($-CH_3$). ^{31}P-NMR (298 K, 125 MHz, CDCl$_3$, ppm): δ 10.02.

P2-H. ^{1}H-NMR (298 K, 300 MHz, CDCl$_3$, ppm): δ 3.96 (qd, 6H, $-O-CH_2-$), δ 1.66 (dtt, 6H, $-O-CH_2-CH_2-$), δ 1.40–1.20 (m, 26H, $-CH_2-$), δ 0.93 (t, $J = 6$ Hz, 3H, $-CH_3$). ^{13}C-NMR (298 K, 75 MHz, CDCl$_3$, ppm): δ 67.15 ($-O-CH_2-$), 38.18 ($-O-CH_2-CH_2-$), 29.91 ($-CH_2-$), 25.95 ($-CH_2-CH_3$), 19.15 ($-CH_2-CH_3$), 14.31 ($-CH_3$). ^{31}P-NMR (298 K, 125 MHz, CDCl$_3$, ppm): δ −0.84.

Procedure for the selective degradation of amidate side chain. Into a NMR tube were added 5 mg of **poly(1)** and 5 mg of *p*-toluenesulfonic acid in a mixture of deuterated chloroform and deuterated methanol (6:4). The degradation was measured every day over the duration of 1.5 weeks by ^{1}H NMR and ^{31}P NMR spectroscopy.
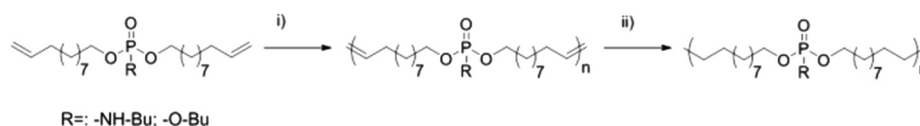
Results and discussion

For the comparison of PPEs with PPAs, we designed two novel α,ω-dienes, *i.e.* bis-(undecen-10-yl) butylphosphoramidate (**1**) and its phosphoester equivalent (**2**) (characterization data can be found in the ESI†). Both monomers can be synthesized starting from phosphoroxychloride with sequential substitution of the chlorides with alcohols (10-undecen-1-ol and/or *n*-butanol) and/or the amine (*n*-butylamine) (Scheme 1). Due to its high nucleophilicity, the amine is attached after the incorporation of the polymerizable groups, while for the phospho-

ester side chain (**2**) butanol can be also added in the first step. Both monomers were purified by column chromatography and are stable at room temperature over a period of at least several months (^{1}H, ^{13}C, ^{31}P, [1]H[15]N HMBC NMR spectra can be found in the ESI†). The ^{15}N NMR chemical shift for the amidate-N is detected at 42.3 ppm (Fig. S4†), while the ^{31}P NMR spectra show distinct resonances for the phosphoramidate at *ca.* 10 ppm and the phosphoester at −0.65 ppm (Scheme 1).

Both α,ω-dienes (phosphoramidate/-ester) monomers were polymerized by ADMET polycondensation using the 1st generation Grubbs catalyst or the 2nd generation Hoveyda–Grubbs catalyst. The reaction was carried out in bulk at 80 °C for 12 h at reduced pressure in order to remove the ethylene evolved during this reaction (Scheme 2). For the poly(phosphoramidate)s polymerization by the 1st generation Grubbs catalyst (3 mol%) produced polymers with apparent M_n's of up to 4800 g mol^{-1}. The polymerization of **1** was also investigated with the typically more active 2nd generation Grubbs–Hoveyda catalyst. 1, 3, 5, and 10 mol% were used and the apparent M_n values were increased to *ca.* 9000 g mol^{-1} for 5 mol% catalyst loading. 10 mol% of catalyst loading changed the molar mass only slightly (Table 1 & Fig. S14†). In addition to SEC, apparent molecular weights have been determined by ^{1}H DOSY NMR spectroscopy for two examples: ^{1}H-DOSY NMR. In order to determine M_w of the polymers, poly(styrene) samples with known absolute molecular weights (GPC standards) were measured *via* DOSY and used as a calibration.[27,28] The determined M_ws from the H-DOSY NMR spectra are in a range between 9400 g mol^{-1} and 11 000 g mol^{-1} for the PPAs **P1-b** and **P1-d**, respectively.

The poly(phosphoester) based on **2** was not reported in the literature, however similar polymers with phenoxy side chains have been prepared and GPC indicates for **P2**s a M_n of *ca.* 9000 g mol^{-1} in this case (which is probably not the upper limit). Successful polymerization of both monomers can be easily detected from the ^{1}H NMR spectra, as the terminal olefin resonances change into internal alkenes after the polymerization (end groups may be detected, but isomerization is known to shift the end groups also to internal alkenes, spectra can be found in the ESI†). These unsaturated PPAs/PPEs converted by catalytic hydrogenation with Pd/C into their saturated counterparts. The ^{1}H NMR spectra show the disappearance of any alkene resonances after successful hydrogenation (Fig. S11 & S12†) and SEC proves the stability of the polymer under these conditions (Fig. S16†).

As possible flame-retardant materials phosphoramidates typically exhibit different thermal behavior compared to their ester analogues.[25] The thermal properties of the unsaturated

Scheme 2 ADMET polymerization of **1** and **2** and subsequent hydrogenation (i) Grubbs catalyst, vacuum, 60−80 °C; (ii) Pd/H$_2$, toluene).

Table 1 Characterization data for poly(phosphoramidate)s **P1** and poly(phosphoester)s **P2**

Code	Conditions[a]	M_n[b]	M_w/M_n[b]	T_g[c]/°C	T_m[c]/°C
P1-a	A	3100	1.25	n.d.	n.d.
P1-b	A	4800	2.19	−72	−8
P1-c	B	4400	1.82	n.d.	n.d.
P1-d	C	6500	1.70	−71	8
P1-e	D	9000	1.72	n.d.	n.d.
P1-f	E	9500	1.66	n.d.	n.d.
P1-g	F	14 000	2.01	n.d	n.d.
P2-a	A	9000	2.70	−84	0
P2-b	A	9600	2.71	n.d.	n.d.
P2-c	D	19 600	1.81	n.d.	n.d.
P1-d-H	—	7000	1.60	−50	51
P2-b-H	—	10 000	2.55	−80	47

[a] A: 1st generation Grubbs, 3 mol%, 24 h. 2nd gen. Grubbs–Hoveyda. 1 mol%, 24 h = B; 3 mol%, 24 h = C; 5 mol%, 24 h = D; 10 mol%, 24 h = E; 5 mol%, 48 h = F. [b] Determined *via* SEC in THF (*vs.* PS standards). [c] Determined by differential scanning calorimetry (10 K min⁻¹). n.d. = not determined.

and saturated poly(phosphoramidate)s and poly(phosphoester)s were studied by differential scanning calorimetry (DSC) and thermogravimetric analysis (TGA) (Fig. S17 & S18†). **P2** was studied by TGA and single thermal decomposition at *ca.* 310 °C (10% weight loss: $T_{10\%}$ = 311 °C) with a char residue at 450 °C of 9% was observed. The thermal degradation of phosphoramidates is different compared to phosphoesters and was already studied for various flame retardant additives or modified polymers (typically with low molecular weight additives or modification of a common polymer matrix).[29,30] **P1** shows a more complex degradation profile than the corresponding polyester: a first mass loss of *ca.* 23% mass up to *ca.* 298 °C, followed by a second process until *ca.* 325 °C and 60% weight loss. This char slowly degrades under further heating to *ca.* 15% remaining at 440 °C. Compared to low molecular weight flame retardant phosphoramidates, this TGA profile also makes PPAs interesting candidates for flame retardants additives.[25]

The hydrogenated samples (**P1-H** and **P2-H**) can also be regarded as a defective poly(ethylene) (PE) with the phosphate-/amidate acting as defects, spaced by 20 methylene groups. The unsaturated PPE (**P2**) shows a low T_g of *ca.* −84 °C and a melting endotherm at *ca.* 0 °C with a melting enthalpy of ΔH_m = −31 J g⁻¹. After hydrogenation (**P2-H**), the T_g remains rather unchanged (−80 °C) and the melting temperature is increased to *ca.* 47 °C (ΔH_m = −59 J g⁻¹), similar to previously reported PPEs.[21,31] Interestingly, a second melting endotherm is detected after hydrogenation at *ca.* −1 °C with a very low ΔH_m = −8 J g⁻¹, indicating another crystalline structure, which may be due to side chain crystallinity (Fig. S18†). For the unsaturated PPAs **P1** a different behavior is detected: the T_g is −72 °C higher than that for the corresponding PPE; in addition above T_g the polymer crystallizes at T_c = −40 °C, before the melting is detected at −8 °C. Also in the cooling curve of the **P1**-series, no recrystallization is observed under these conditions (10 °C min⁻¹), leaving a completely amorphous polymer after cooling. In contrast, **P2** recrystallizes during the same cooling procedure. The hydrogenated PPA (**P1-H**) exhibits a similar thermal behavior as its PPE-analog with a melting endotherm at *ca.* 51 °C with a similar melting enthalpy of ΔH_m = −45 J g⁻¹.

The solid state properties of **P1-H** and **P2-H** were analyzed by WAXS and SAXS measurements. The small angle X-ray scattering diagram (Fig. 1) shows a dominant peak at q = 0.2368 Å⁻¹, corresponding to a long period of 2.7 nm. This peak is found in the wide angle X-ray scattering (WAXS) as well at 2Θ = 3.6°. Accordingly, the lamellar thickness of **P1-H** crystals corresponds to the length of the 20 CH₂ groups in all-*trans* conformations. **P1-H** and **P2-H** were dissolved in hot *n*-octane and crystallized slowly during the cooling process from solution. Drop-cast TEM (*cf.* Fig. S19 & S20†) shows the resulting crystals for both polymers. The electron diffraction pattern (inset Fig. S19 and S20†)) indicates that the crystal packing is similar to the pseudohexagonal crystal phase of polyethylene.[32] For **P1-H** a lattice spacing of 4.1 Å was measured from TEM diffraction and also the WAXS measurement yields a lattice spacing of 4.1 Å. Interestingly, the structural analogue of PPE, *i.e.* **P2-H**, behaves similarly in the bulk phase: the SAXS diagram (Fig. S21†) shows a major signal at q = 0.2808 Å⁻¹, corresponding to a long period of 2.2 nm, similar to **P1-H**. The WAXS shows a small peak at 2Θ = 6.8° which corresponds to a spacing of 1.3 nm. The dominant peak in the WAXS data
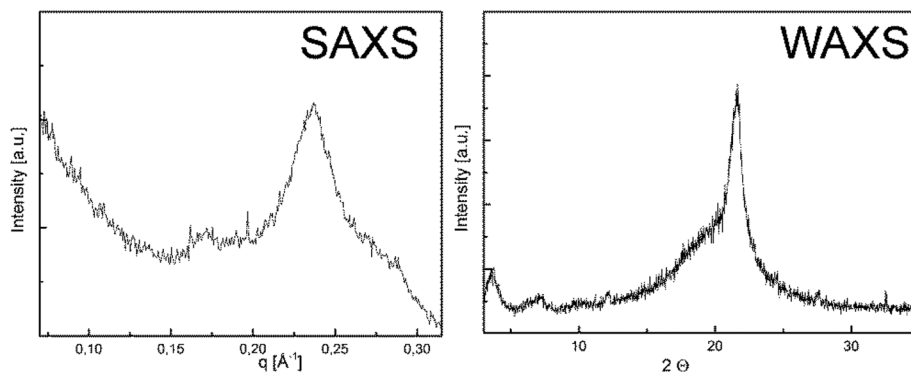

Fig. 1 Small- and wide angle X-ray scattering of **P1-H**. Prior to the X-ray measurement the sample was annealed at 42 °C for 24 hours.
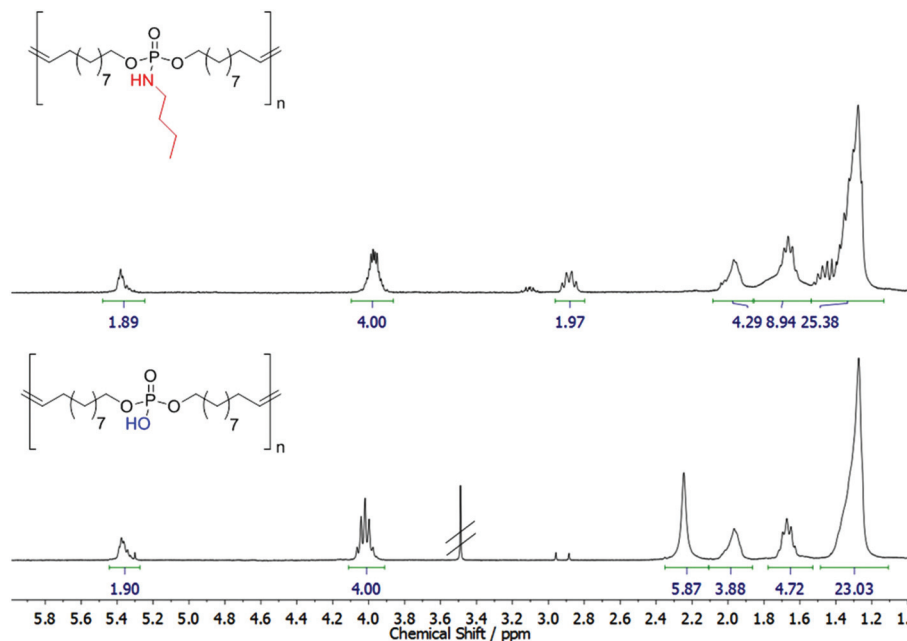
Fig. 2 Degradation of **P1** and preparation of a poly(phosphodiester). Top: ^{1}H NMR of **P1**. Bottom: ^{1}H NMR of degraded **P1**.

corresponds to a lattice spacing of 4.2 Å, indicating again the pseudo-hexagonal crystal structure. Fig. S20† shows a TEM micrograph of **P2-H** crystals with the corresponding diffraction pattern yielding a lattice spacing of 4.2 Å (compare above 4.1 Å for **P1-H**). From these structural examinations the **P2-H** crystallizes in a pseudo-hexagonal crystal structure with a lamellar long period of 2.2 nm as **P1-H**. As reported previously for other defect-PEs, the pendant groups are located outside the crystalline lamellae[33] and thus for **P1-H** the amidate side chains are located outside the crystals. Due to the easy cleavage of P–N bonds (see below), this might be a handle for future tuning of crystal surfaces and currently studied in our department.

The P–N-bond in phosphoramidates is known to be hydrolytically labile in contrast to the stronger P–O bond.[13] Thus, PPAs can be used to release the pendant groups in an acidic environment; while at neutral pH PPAs are stable. This behavior makes PPAs advantageous for using in a low pH-triggered release of the side chain-bound material, *e.g.* for drug release.

The cleavability of the phosphoramidate bond with *p*-toluenesulfonic acid was investigated by ^{1}H NMR (Fig. 2) and ^{31}P NMR (Fig. S13†): the complete conversion of the phosphoramidate (9.78 ppm) into a phosphate group (0.40 ppm) was detected after 7 days. No scission of the main chain was observed under these conditions from the NMR spectra. It has to be noted that the polyphosphodiester exhibits low solubility in common solvents (either methanol/chloroform mixtures or basic conditions, *e.g.* pyridine, can be used), and thus SEC analysis was not possible. However, literature reports show that phosphodiesters have a very high stability under acidic conditions.[34] This makes the pendant amidate also

a potential protective group for the P–OH group, which allows easy handling due to higher solubility as the resulting polyphosphodiester.

Conclusions

In summary, this work presented the first synthesis of poly(phosphoramidate)s *via* acyclic diene metathesis polycondensation. In addition the comparison of structural analogues of saturated and unsaturated poly(phosphoester)s was performed. Distinct differences for both classes of materials have been identified based on their thermal behavior, thermal stability, and hydrolytic stability. Their crystallization behavior was found to be very similar and rather independent of the binding motif of the pendant chain. The pendant amidate was selectively hydrolyzed under acidic conditions, producing a poly(phosphodiester) with a very high stability towards acids. This selective degradation profile makes phosphoramidates a powerful protective group for P–OH groups, which in general exhibit strong hydrogen bonding and low solubility. These materials extend the class of degradable P-containing polymers that may find applications ranging from fire retardant additives to biodegradable scaffolds for tissue engineering or drug delivery.

Acknowledgements

References

1 J. Wang, P. Zhang, H. Mao and K. Leong, *Gene Ther.*, 2002, **9**, 1254–1261.

2 S.-W. Huang and R.-X. Zhuo, *Phosphorus, Sulfur Silicon Relat. Elem.*, 2008, **183**, 340–348.

3 Y. Ikada and H. Tsuji, *Macromol. Rapid Commun.*, 2000, **21**, 117–132.

4 T. Steinbach and F. R. Wurm, *Angew. Chem., Int. Ed.*, 2015, **54**, 6098–6108.

5 Y. H. Lim, G. S. Heo, Y. H. Rezenom, S. Pollack, J. E. Raymond, M. Elsabahy and K. L. Wooley, *Macromolecules*, 2014, **47**, 4634–4644.

6 Z. Zhao, J. Wang, H.-Q. Mao and K. W. Leong, *Adv. Drug Delivery Rev.*, 2003, **55**, 483–499.

7 F. Zhang, S. Zhang, S. F. Pollack, R. Li, A. M. Gonzalez, J. Fan, J. Zou, S. E. Leininger, A. Pavía-Sanders, R. Johnson, L. D. Nelson, J. E. Raymond, M. Elsabahy, D. M. P. Hughes, M. W. Lenox, T. P. Gustafson and K. L. Wooley, *J. Am. Chem. Soc.*, 2015, **137**, 2056–2066.

8 F. Zhang, J. A. Smolen, S. Zhang, R. Li, P. N. Shah, S. Cho, H. Wang, J. E. Raymond, C. L. Cannon and K. L. Wooley, *Nanoscale*, 2015, **7**, 2265–2270.

9 J. Wang, H.-Q. Mao and K. W. Leong, *J. Am. Chem. Soc.*, 2001, **123**, 9480–9481.

10 J.-J. Qiu, C.-M. Liu, F. Hu, X.-D. Guo and Q.-X. Zheng, *J. Appl. Polym. Sci.*, 2006, **102**, 3095–3101.

11 K. N. Bauer, H. T. Tee, I. Lieberwirth and F. R. Wurm, *Macromolecules*, 2016, **49**, 3761–3768.

12 T. Wolf, T. Steinbach and F. R. Wurm, *Macromolecules*, 2015, **48**, 3853–3863.

13 S. Zhang, H. Wang, Y. Shen, F. Zhang, K. Seetho, J. Zou, J.-S. A. Taylor, A. P. Dove and K. L. Wooley, *Macromolecules*, 2013, **46**, 5141–5149.

14 J. Wang, S. J. Gao, P. C. Zhang, S. Wang, H. Q. Mao and K. W. Leong, *Gene Ther.*, 2004, **11**, 1001–1010.

15 K. Troev, I. Tsatcheva, N. Koseva, R. Georgieva and I. Gitsov, *J. Polym. Sci., Part A: Polym. Chem.*, 2007, **45**, 1349–1363.

16 V. Mitova, N. Koseva and K. Troev, *RSC Adv.*, 2014, **4**, 64733–64736.

17 X.-Q. Zhang, X.-L. Wang, S.-W. Huang, R.-X. Zhuo, Z.-L. Liu, H.-Q. Mao and K. W. Leong, *Biomacromolecules*, 2005, **6**, 341–350.

18 X. Jiang, W. Qu, D. Pan, Y. Ren, J.-M. Williford, H. Cui, E. Luijten and H.-Q. Mao, *Adv. Mater.*, 2013, **25**, 227–232.

19 W. Batorewicz, Uniroyal Inc., *US Pat.*, US3932565-A, 1976.

20 T. Steinbach, C. Wahlen and F. R. Wurm, *Polym. Chem.*, 2015, **6**, 1192–1202.

21 T. Steinbach, E. M. Alexandrino, C. Wahlen, K. Landfester and F. R. Wurm, *Macromolecules*, 2014, **47**, 4884–4893.

22 T. Steinbach, E. M. Alexandrino and F. R. Wurm, *Polym. Chem.*, 2013, **4**, 3800–3806.

23 H. Mutlu, L. M. de Espinosa and M. A. R. Meier, *Chem. Soc. Rev.*, 2011, **40**, 1404–1445.

24 S. A. Low and J. Kopeček, *Adv. Drug Delivery Rev.*, 2012, **64**, 1189–1204.

25 M. Neisius, S. Liang, H. Mispreuve and S. Gaan, *Ind. Eng. Chem. Res.*, 2013, **52**, 9752–9762.

26 A. Jerschow and N. Müller, *J. Magn. Reson., Ser. A*, 1996, **123**, 222–225.

27 W. Li, H. Chung, C. Daeffler, J. A. Johnson and R. H. Grubbs, *Macromolecules*, 2012, **45**, 9595–9603.

28 M. Mazarin, S. Viel, B. Allard-Breton, A. Thévand and L. Charles, *Anal. Chem.*, 2006, **78**, 2758–2764.

29 T.-M. Nguyen, S. Chang, B. Condon, R. Slopek, E. Graves and M. Yoshioka-Tarver, *Ind. Eng. Chem. Res.*, 2013, **52**, 4715–4724.

30 S. Gaan, P. Rupper, V. Salimova, M. Heuberger, S. Rabe and F. Vogel, *Polym. Degrad. Stab.*, 2009, **94**, 1125–1134.

31 F. Marsico, M. Wagner, K. Landfester and F. R. Wurm, *Macromolecules*, 2012, **45**, 8511–8518.

32 W. Qiu, J. Sworen, M. Pyda, E. Nowak-Pyda, A. Habenschuss, K. B. Wagener and B. Wunderlich, *Macromolecules*, 2006, **39**, 204–217.

33 Y. R. Zheng, H. T. Tee, Y. Wei, X. L. Wu, M. Mezger, S. Yan, K. Landfester, K. Wagener, F. R. Wurm and I. Lieberwirth, *Macromolecules*, 2016, **49**, 1321–1330.

34 A. J. Kirby and M. Younas, *J. Chem. Soc. B*, 1970, 510–513.